THE JOURNAL OF PHYSICAL CHEMISTRY B

Article

Cite This: J. Phys. Chem. B 2018, 122, 1112−1120

pubs.acs.org/JPCB

Specificity versus Processivity in the Sequential Modification of DNA: A Study of DNA Adenine Methyltransferase

Itay Barel,[†,‡] Brigitte Naughton,[†] Norbert O. Reich,[†] and Frank L. H. Brown*[,†,‡]

[†]Department of Chemistry and Biochemistry, University of California, Santa Barbara, California 93106, United States

[‡]Department of Physics, University of California, Santa Barbara, California 93106, United States

ABSTRACT: A detailed analysis is carried out on both published experimental results and new experiments for the methylation kinetics of two-site DNA substrates (with site separations between 100 and 800 bp) catalyzed by bacterial DNA adenine methyltransferase (Dam). A previously reported rate enhancement for the second methylation event (relative to that of the first methylation) is shown to result from elevated substrate specificity for singly methylated DNA over that of unmethylated DNA and *not* processive turnover of both sites by the same copy of Dam. An elementary model is suggested that cleanly fits the experimental data over a broad range of intersite separations. The model hypothesizes a looping mediated interference between competing unmethylated Dam sites on the same DNA strand.

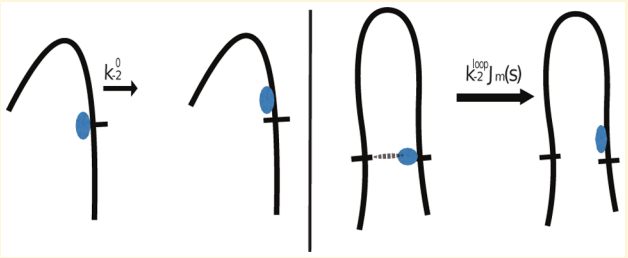

1. INTRODUCTION

The interaction of proteins and DNA plays a crucial role in many aspects of cellular function. Gene transcription, packing/unpacking DNA into chromosomes, mismatch repair, and epigenetic gene regulation all rely upon protein−DNA interactions; these regulatory and structural functions are often interwoven.[1−8] Understanding the kinetics of protein−DNA interactions is essential to the detailed mechanistic understanding of cellular function.

A fundamental and persistent puzzle common to many aspects of DNA−protein interaction is the uncanny ability of proteins to locate specific target sites along the DNA chain with remarkable speed and fidelity, often without the consumption of chemical energy. Although great effort has been expended to understand this process for more than 40 years (see, for example, refs 9−19 and references within), complete understanding remains elusive with controversy persisting to this day.[20−24] A popular approach to study enzyme translocation and target localization on DNA involves the investigation of turnover kinetics of DNA substrates engineered with two recognition sites selectively placed along the DNA chain.[10,16,20,25−27] The turnover rates for these sites as a function of site location, intersite spacing, overall DNA length, and various thermodynamic conditions (e.g., salt concentrations) provide valuable information to test hypothetical mechanisms for enzymatic activity in these complicated macromolecular systems.

In recent work,[28] some of the present authors reported the methylation kinetics of two-site DNA constructs by bacterial DNA adenine methyltransferase (Dam). An unambiguous experimental observation in that work was faster turnover kinetics for the second methylation event than for the first methylation when intersite separations were well suited to DNA looping.[29,30] However, these experiments were interpreted using the traditional assumption[25] that the relatively faster second methylation is driven by processive turnover; i.e., the same copy of Dam responsible for the first methylation can remain bound to the DNA substrate to effect the second methylation as well. Although this assumption is commonplace and seemed quite plausible, it was not justified by any measurement or other direct evidence. The primary point of this paper is to demonstrate that Dam acts in essentially a nonprocessive fashion on the considered substrates (with target sites separated by over 100 bp), contrary to the original analysis and requiring a revised mechanism to consistently explain the experimental data. This provocative claim follows from a powerful new method of data analysis,[31] which is briefly summarized below.

A general steady-state analysis of enzymatic turnover of two-site substrate systems has recently been carried out.[31] One practical outcome of this analysis is the simple expression for two kinetically identical turnover sites on a single substrate molecule

$$\frac{d[S]/dt}{d[U]/dt} = \frac{C_{sp}^{S\to D}}{C_{sp}^{U\to S}}\frac{[S]}{[U]} - (1 - f_p) \quad (1)$$

Here, U, S, and D are substrate/product species that are, respectively, unmodified, singly modified, or doubly modified from their starting form. In this work, U, S, and D represent unmethylated, singly methylated, and doubly methylated DNA and the catalyst for the reaction is the enzyme Dam. f_p is the

Received: October 22, 2017
Revised: December 19, 2017
Published: December 19, 2017

DOI: 10.1021/acs.jpcb.7b10349
J. Phys. Chem. B 2018, 122, 1112−1120

"fraction processive"[16] or processivity of the turnover reaction. f_p is the probability that the full conversion process U → S → D of an individual DNA molecule proceeds via a single enzyme binding event; i.e., a single copy of the enzyme processively methylates both target sites on the DNA. $C_{sp} = \frac{k_{cat}}{K_M}$ denotes specificity constants[32] for the indicated individual turnovers (U → S or S → D).

Equation 1 has been derived in the context of arbitrarily complicated reaction mechanisms under a very modest set of assumptions.[31] In short, eq 1 is as general as is the Michaelis–Menten rate law for single-site substrates. Thus, in the same way that it is possible to extract values of k_{cat} and K_M from a linear Lineweaver–Burk or Eadie–Hofstee plot for a traditional single-site substrate with unknown mechanistic details,[33,34] eq 1 allows a model-free determination of f_p and $\frac{C_{sp}^{S\to D}}{C_{sp}^{U\to S}}$ directly from a linear plot of experimental data (see section 3.1). The generality of the approach allows it to be used to study DNA substrates which involve all manners of enzyme translocation mechanisms along the DNA chain (e.g., sliding,[9,35] hopping,[10,36−38] intersegmental transfer,[28,35,36,39−42] etc.) and complex multistep chemical conversions; it was with these complications specifically in mind that the theory was developed. The prediction has been extensively tested against complex kinetic schemes[31] and yields f_p results identical to initial rate values,[10] when used to interpret experimental data that is amenable to both forms of analysis.[16,31]

However, eq 1 has two important advantages over a traditional initial-rates approach to determination of f_p. First, the expression is valid over the entire course of the reaction; it is not limited to early times. Second, analysis of experiment based on eq 1 provides both f_p and the ratio of specificity constants, $\frac{C_{sp}^{S\to D}}{C_{sp}^{U\to S}}$. In the case of Dam, it will be shown that the interesting mechanistic information is held in the ratio $\frac{C_{sp}^{S\to D}}{C_{sp}^{U\to S}}$ and not f_p—a result that would have gone unnoticed in an initial-rates measurement.

It was originally hoped that the raw experimental data from ref 28 could be reanalyzed with eq 1 to provide an unbiased measurement of f_p; however, this proved impossible.[31] The data collected in ref 28 did not anticipate analysis via eq 1; [U](t) and [S](t) were sampled nonsystematically and too sparsely in time to allow the rates d[U]/dt and d[S]/dt to be meaningfully estimated over the course of the reaction.

In this work, two of the original experiments from ref 28 have been repeated with a higher time resolution and greater precision. This allows direct application of eq 1, with results that unambiguously indicate nonprocessive turnover of the two-site constructs. Although this finding completely invalidates a key assumption of the original analysis, it is stressed that the new experiments reported here are fully consistent with those of the original study.[28] The new data is simply "cleaner" and better suited for the refined analysis that allows an unbiased and model-free determination of f_p; it was collected expressly for this purpose.

The organization of this paper is as follows. In sections 2 and 3.1, the new activity based assays for Dam methylation of two-site DNAs are presented and interpreted via eq 1. These results clearly contradict the assumptions of the analysis in ref 28, requiring a revised explanation for both the original and new experiments. A mechanism is proposed in section 3.2 that explains all of the experimental results (seven different DNA constructs with intersite separations ranging between 134 and 798 bp) in the framework of a six-state kinetic scheme. (The appendix shows that these kinetics can be simplified to an effective four-state scheme to provide simpler mathematical expressions at the expense of some chemical details.) The comparison between experiment and model is detailed in sections 3.3 and 3.4.

2. METHODS

The majority of the experimental data analyzed in sections 3.3 and 3.4 was collected previously (though not reported in raw form) in ref 28 as the "4B" data set from that work. Details of the experimental procedures may be found in the "Processivity Assay" section of that work, and details of the specific DNA fragments studied may be found in section 1 and Table S1 of the Supporting Information for that work. In brief, the experiments all involve engineered DNA substrates with two Dam methylation sites placed symmetrically along the chain, which are assumed to behave kinetically identical to one another (see Figure 1). The measurements quantify the time-dependent concentration of unmethylated DNA, [U](t); singly methylated DNA, [S](t); and doubly methylated DNA, [D](t), starting at t = 0 with the introduction of 7 nM Dam to a solution of 400 nM unmethylated DNA, 30 μM AdoMet (*S*-adenosyl methionine), 29.3 mM NaCl, 100 mM Tris–HCl (pH 8.0), 0.23 mM EDTA (ethylenediaminetetraacetic acid), 0.23

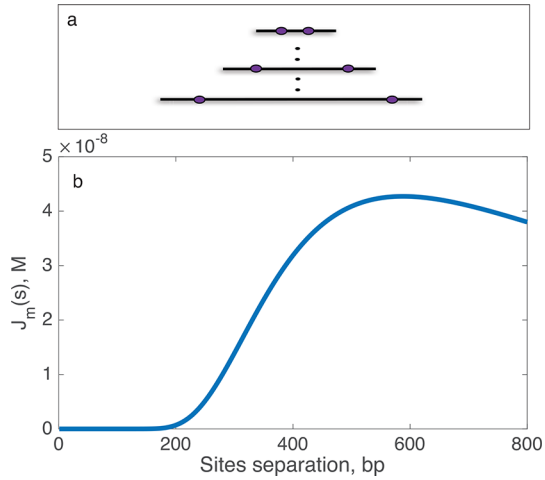

Figure 1. (a) The DNA constructs studied in this work correspond to the "4B" set of DNAs from ref 28. These DNAs all involve two Dam methylation sites flanked at the edges by 115 and 119 bp of DNA. The constructs differ from one another through the intersite distance, s, which is varied from 134 to 798 bp. The new experiments reported in this work are specific to s = 134 bp and s = 482 bp. Data for the other constructs discussed in sections 3.3 and 3.4 was obtained in ref 28. (b) Plot of the function $J_m(s)$[30,43,44] as a function of the distance between the methylation sites. (See eq 4.) $J_m(s)$ reports the average equilibrium concentration of one site around the other due to thermal fluctuations of DNA shape. Equivalently, $J_m(s)$ is proportional to the equilibrium probability for DNA to loop back on itself, placing the two methylation sites in proximity. This probability is practically zero for site separations smaller than the DNA persistence length (150 bp), peaks at intersite distances approximately 500–600 bp from each other, and then shows a gentle drop as the intersite distance continues to increase.

DOI: 10.1021/acs.jpcb.7b10349
J. Phys. Chem. B 2018, 122, 1112−1120

mM DTT (dithiothreitol), and 0.27 mg/mL BSA (bovine serum albumin), run at 37 °C. Samples at individual time points were heat quenched with 80 °C deionized water and subsequently digested with excess DpnII ENase to cut unmethylated GATC sites for PAGE analysis. The slowest migrating band represents uncut (doubly methylated, D) species; the middle band is singly methylated DNA (S), and the bottom band, lacking methylation, is doubly cut (unmethylated, U).

As mentioned in the Introduction, this data lacks the required time resolution and precision to carry out the model-free analysis for f_p and $\frac{C_{sp}^{S\to D}}{C_{sp}^{U\to S}}$ based on eq 1. To enable this analysis, two of the previously studied DNAs were chosen for remeasurement in this work: sample 4B-2, a 368bp DNA with Dam target sites separated by 134 bp, and sample 4B-8, a 716 bp DNA with Dam target sites separated by 482 bp. These particular DNA substrates were chosen because they represent an apparently weakly processive case (4B-2) and an apparently strongly processive case (4B-8) as inferred through the original analysis in ref 28. Experimental conditions and protocols for the present work are identical to those presented in ref 28 and summarized above; the only difference in the new experiments is that reaction progress was sampled at precise 5 min intervals as opposed to the more haphazard sampling of the original study. The well-specified sampling interval allowed each experiment to be repeated six times and averaged to lower uncertainty.

3. RESULTS

3.1. Model-Free Determination of f_p and the Specificity Constant Ratio. The results of the previously unpublished measurements described in section 2 are displayed in Figure 2. Figure 3 plots these results on suitable axes to allow

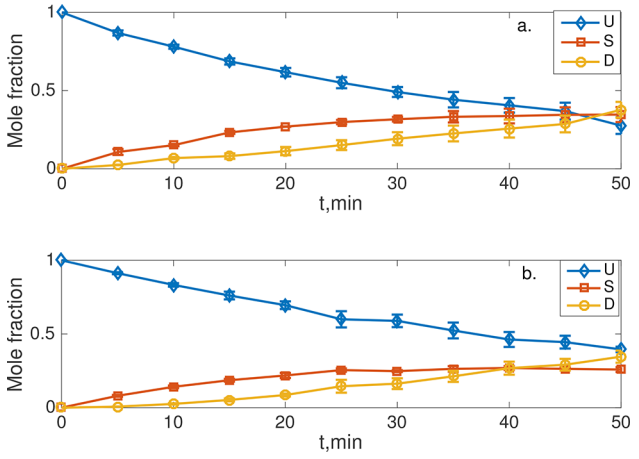

Figure 2. Unmethylated (blue diamonds), singly methylated (red squares), and doubly methylated (yellow circles) DNA populations as a function of time for (a) 368 bp DNA with active sites separated by 134 bp (this is the same DNA construct as 4B-2 of ref 28) and (b) 716 bp DNA with active sites separated by 482 bp (the same construct as 4B-8 of ref 28). The solid lines have been added for clarity. The results reflect averaging over six repetitions of the experiment for each construct, and the error bars indicate the associated standard deviations. These are previously unpublished results, repeating the measurements from ref 28 with higher time resolution and better precision.

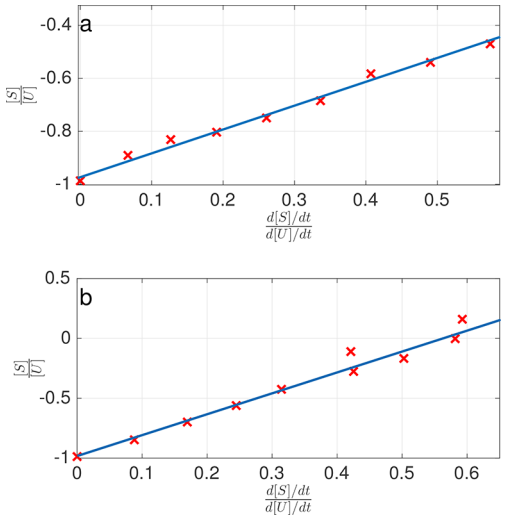

Figure 3. Linear fits of the experimental data (see Figure 2) to eq 1. The parameters obtained for the 368 bp (134 bp site separation) DNA sample (panel a) are $f_p = 0.01 \pm 0.03$, $\frac{C_{sp}^{S\to D}}{C_{sp}^{U\to S}} = 0.90 \pm 0.05$ and for the 716 bp (482 bp site separation) DNA sample (panel b) $f_p = 0.02 \pm 0.04$, $\frac{C_{sp}^{S\to D}}{C_{sp}^{U\to S}} = 1.85 \pm 0.06$.

comparison to eq 1 with f_p and $\frac{C_{sp}^{S\to D}}{C_{sp}^{U\to S}}$ following from the intercept and slope of linear fits. While the experimental data follows the theoretical prediction nearly perfectly, two surprising results arise from the data analysis. First, both DNA samples show an intercept close to −1, meaning that both constructs are only very slightly processive. (Within the uncertainty of the data, both cases may be entirely non-processive.) This finding directly contradicts the interpretation/analysis of the original experiments presented in ref 28, which predicted both cases were processive and a particularly high processivity for the 716 bp construct. (The flawed analysis method from ref 28 was applied to the new experimental data and yielded conclusions similar to the original analysis. The new data presented here is entirely consistent with the original experiments; however, only the new data is suited for the robust model-free analysis described in this section.) Second, the two constructs return significantly different slopes to the linear fits, translating into different specificity constant ratios ($\frac{C_{sp}^{S\to D}}{C_{sp}^{U\to S}}$) for the two cases. The ratio for the 716 bp DNA sample (1.85) is more than double that of the 368 bp construct (0.90). This means that Dam favors the S → D turnover relative to the U → S turnover in the longer construct absent any processivity but is nearly indifferent between the two turnovers in the shorter construct.

The analysis of ref 28 incorrectly assumed (following literature precedent[25]) that any observed enhancements to the velocity of S → D relative to U → S were due to processive turnover events. The present analysis shows that the relatively greater speed of the second turnover is, in fact, due to a specificity effect. The flawed analysis of ref 28 attributed the anomalously high S → D velocity (equivalently, the anomalously low U → S velocity) to processive turnover because that was the only possibility allowed in the analysis.

3.2. Proposed Mechanism: Intersegmental Facilitated Dissociation. One obvious limitation to analysis based on eq 1

DOI: 10.1021/acs.jpcb.7b10349
J. Phys. Chem. B 2018, 122, 1112−1120

is that the turnover specificity constants are obtained only in ratio to one another and not individually. On the basis of Figure 3 alone, it is thus impossible to guess whether the second methylation event is accelerated relative to the first in the 716 bp sample or whether the first methylation event is being inhibited relative to the second. Individual turnover information is not available for comparison against a reference situation, and both cases would lead to $\frac{C_{sp}^{S\to D}}{C_{sp}^{U\to S}} > 1$. However, the raw data displayed in Figure 2 contains information beyond that used in eq 1. In particular, it is clear that the overall reaction rate for the 716 bp sample is slower than that for the 368 bp construct and the slowing appears to be caused predominately by the U → S turnover. This trend persists throughout the entire 4B data set of ref 28 (see Table S1 of the Supporting Information to ref 28); the constructs with larger intersite spacings display slower U → S turnover kinetics than do constructs with smaller intersite spacings. The S → D turnovers are, in contrast, uncorrelated with intersite separation.

A key insight from ref 28 is that the turnover kinetics of Dam on two-site substrates are closely correlated with the DNA looping probability (Figure 1) between the two sites. Taken together with the details outlined in the previous paragraph and the nonprocessive nature of the consecutive turnovers verified in section 3.1, the following hypothetical picture of Dam methylation kinetics emerges. U → S turnover by Dam is slowed by interference from the second methylation site when the two sites are brought into proximity via looping. This interference is not present in the S → D case when the second site is already methylated. A concrete realization of this picture is provided by the kinetic scheme

$$E+U \underset{k_{-1}}{\overset{k_1(L)}{\rightleftharpoons}} EU \underset{k_{-2}(s)}{\overset{k_2}{\rightleftharpoons}} EU^{specific} \xrightarrow{k_3} E+S \qquad (2)$$

$$\downarrow k_{sp}$$

$$E+S \underset{k_{-4}}{\overset{k_4(L)}{\rightleftharpoons}} ES \underset{k_{-5}}{\overset{k_5}{\rightleftharpoons}} ES^{specific} \xrightarrow{k_6} E+D \underset{k_{-7}}{\overset{k_7(L)}{\rightleftharpoons}} ED$$

Here, Dam (E) binds to unmethylated DNA (U) to create a nonspecific complex EU; the binding rate depends on the amount of DNA available to bind to through the total DNA length L. From there, Dam can either be released back to the solution without catalyzing a reaction, or it can find one of the two equivalent target sites to form the specific complex $EU^{specific}$. There are three posited pathways out of $EU^{specific}$. Dam either releases the target to return to EU or methylates the DNA to create singly methylated DNA (S). The turnover results in either immediate release of S to solution or a potentially processive event where Dam remains on the DNA and finds the second target site in the complex $ES^{specific}$. Turnover of S is qualitatively similar to that of U, resulting in doubly methylated product D. The effect of DNA looping is captured in the rate constant $k_{-2}(s)$ that is assumed to be a function of the intersite spacing s as

$$k_{-2}(s) = k_{-2}^{0} + k_{-2}^{loop} J_m(s) \qquad (3)$$

with

$$J_m(s) = \left(\frac{3}{4\pi s L_p}\right)^{3/2} \times e^{(-8L_p{}^2/s^2)} \times (46.22 Mbp^3) \qquad (4)$$

the effective concentration of the second site around the first due to thermal fluctuations of the DNA chain (i.e., looping).[30,43,44] L_p = 150 bp[10,29] is the persistence length of DNA under the relevant experimental conditions, and the included conversion factor assumes both s and L_p are measured in bp. It is worth emphasizing that L_p is a key physical parameter in this model. Although its value is well-known for the present experimental conditions and is taken as a constant from this point forward, variations in L_p would have a strong effect on the following predictions if experimental conditions were changed (e.g., varying ionic strength[45−50]).

Equation 3 suggests that nonproductive exits from $EU^{specific}$ can result from either "normal" dissociative events from the bound target, that would occur even in single-site DNAs (through k_{-2}^{0}), or through looping mediated "facilitated dissociative" events whereby the unbound unmethylated target encourages dissociation of Dam from the bound target site (through $k_{-2}^{loop}(s)$). Protein-induced facilitated dissociation, i.e., increasing dissociation rates for protein−DNA complexes at higher protein concentration, is a well-known effect in both double stranded DNA[51−53] and single stranded DNA.[54−57] Recent experiments have also demonstrated nonspecific-DNA-induced facilitated dissociation[58] of protein−DNA complexes. Equation 3 describes the possibility of *intramolecular* facilitated dissociation of Dam off the target effected by a competing target site on the same DNA strand, but it can otherwise be viewed as a traditional facilitated dissociation mechanism. Here, the species doing the facilitating is part of the complex that is being dissociated, so the typical bulk concentration is replaced with the effective concentration allowed by looping. The concept of the facilitated dissociation mechanism is illustrated in Figure 4. Note that the facilitated dissociation is assumed to

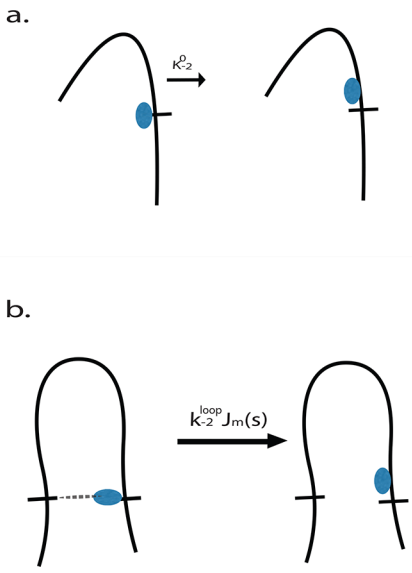

Figure 4. Schematic sketch of the proposed mechanism. (a) For small intersite separations s (shorter then the DNA persistence length), methylation sites are unlikely to be found in proximity to one another. The rate constant for release of Dam from target site to nonspecific DNA is the same as it would be in a single-site construct, k_{-2}^{0}. (b) For DNAs with larger s values, methylation sites can approach each other by looping. This allows an increase in the rate constant for Dam release to nonspecific DNA by means of facilitated dissociation. The total first-order rate constant is $k_{-2}(s) = k_{-2}^{0} + k_{-2}^{loop}J_m(s)$. Note that k_{-2}^{loop} is a second-order rate constant, which becomes a pseudo-first-order rate constant $k_{-2}^{loop}J_m(s)$ when combined with the effective concentration of the unbound site around the bound site.

DOI: 10.1021/acs.jpcb.7b10349
J. Phys. Chem. B 2018, 122, 1112−1120

be possible only in the U DNA state. A previously methylated site does not interfere with the unmethylated site; k_{-5} is assumed to be unaffected by DNA looping and is independent of s.

A natural interpretation of Figure 4 is that EU^{specific} is capable of forming a "ternary" complex involving both target sites with Dam bridging between them. This complex can then unravel, to leave Dam nonspecifically bound. When either of the two sites is methylated, the ternary complex is not formed. However, while this picture is intuitively appealing, it is not supported by detailed molecular analysis tools. DISPLAR[59] finds no alternative DNA binding residues outside the known binding cleft of Dam.[28] Speculation on any molecular details underlying eq 2 cannot be confirmed or refuted on the basis of the experiments discussed in this work, and such speculation is intentionally avoided for the remainder of this paper. The following sections will demonstrate that the proposed kinetic model does an excellent job explaining the available kinetic data without the need to further elaborate on the molecular details underlying eq 2.

The scheme appearing in eq 2 is simple enough to allow fairly concise steady-state solutions.[31] For reference, the relevant results to this study are

$$f_p = \frac{(k_{-4} + k_5)k_6k_p}{(k_{-4}k_{-5} + k_{-4}k_6 + k_5k_6)(k_3 + k_p)}$$

$$C_{sp}^{U\to S} = \frac{k_1k_2(k_3 + k_p)}{k_2(k_3 + k_p) + k_{-1}(k_{-2}(s) + k_3 + k_p)}$$

$$C_{sp}^{S\to D} = \frac{k_4k_5k_6}{k_5k_6 + k_{-4}(k_{-5} + k_6)} \quad (5)$$

The kinetics summarized in eq 2 are speculative but are motivated by the general considerations outlined in the first paragraphs of this section. However, it is important to stress that the proposed scheme is general enough to allow for the possibility of both processive and nonprocessive turnover. At high k_p, the mechanism can be processive, whereas, when k_p = 0, the system is strictly nonprocessive. The following sections 3.3 and 3.4 will show that this mechanism closely fits the full set of data collected in ref 28 (see Figure 5) with only five free parameters. (Although eq 2 indicates 13 rate constants, many of these are known or can be inferred from other experiments.) $k_p \approx 0$ results naturally from this fitting process, providing independent confirmation of the results obtained in section 3.1.

3.3. Limiting the Parameter Space. While the number of rate constants presented in eq 2 appears overwhelming, most of these constants are either known or can be inferred from the behavior of similar DNA−protein systems. This allows a reduction of unknowns to only a handful of parameters that can be fit to the available experimental data.

The rate constants for Dam−DNA association to nonspecific DNA, $k_1(L)$, $k_4(L)$, and $k_7(L)$, are assumed identical to one another and to be proportional to the number of base pairs in a given DNA. Prior studies suggest a generic experimentally motivated value of $k_1 = k_4 = k_7 = 10^5\ s^{-1}\ M^{-1}\ bp^{-1} \times L$[18,60,61] for protein binding to nonspecific DNA. Here, the total DNA length L is measured in base pairs. Similarly, it has been suggested that the rate constant to detach from nonspecific DNA is generically expected to be in the vicinity of $k_{-1} = 10^3\ s^{-1}$,[18,60,61] to yield $K_D = k_{-1}/k_1 = k_{-4}/k_4 = k_{-7}/k_7 = 0.01$ M bp/L. It should be stressed that these choices lead to rates for the nonspecific unbinding/binding steps that are significantly faster than other rates in the problem (see below). The rate limiting steps appear elsewhere in the mechanism, and therefore, it is not critical to make precise assignments for these six rate constants. For convenience, the values of $k_1 = k_4 = k_7$ are provided in Table 2 for each studied construct.

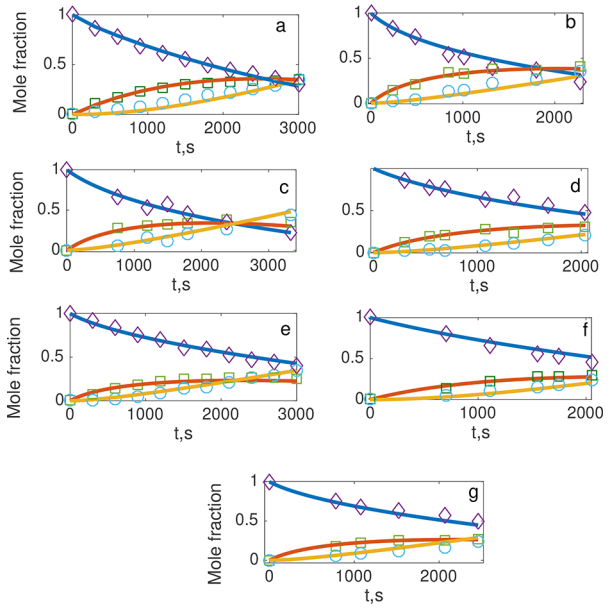

Figure 5. Dam methylation kinetics of DNA with two active sites. Diamonds, squares, and circles represent experimental measurements of [U], [S], and [D], respectively. The solid lines are the result of the numerical evaluation of eq 2 using the best fit parameters of Table 1 and with the remaining rate constants as detailed in section 3.3. The kinetic parameters were fit only to the 716 bp experimental data (panel e) and the same constants used in all of the panes. (a) 368 bp with 134 bp intersite separation (4B-2 from ref 28); (b) 468 bp with 234 bp intersite separation (4B-4); (c) 518 bp with 284 bp intersite separation (4B-5) (high resolution data); (d) 629 bp with 395 bp intersite separation (4B-7); (e) 716 bp with 482 bp intersite separation (4B-8); (f) 839 bp with 605 bp intersite separation (4B-9); (g) 1032 bp with 798 bp intersite separation (4B-10). Note that panels a and e report the previously unpublished data obtained in this work; the remaining panels use data from ref 28. In each case except 4B-9, the repetition was chosen that had behavior closest to the average over all of the repetitions. The data from 4B-9 was far noisier than that for the other constructs, and its average behavior was clearly different from the other constructs. For 4B-9, the repetition with the fastest kinetics was used.

k_{cat} for methylation by Dam is known to be limited by product release with a value of $1.6 \times 10^{-2}\ s^{-1}$.[62] $k_3 = k_6 = 1.6 \times 10^{-2}\ s^{-1}$ are thus assigned to the present study. As discussed in section 3.2, nonproductive release of the target site by Dam can occur via two mechanisms, normal dissociation or facilitated dissociation. It is assumed that normal dissociation is similar in both U and S cases so that $k_{-2}^0 = k_{-5}$.

The remaining five independent rate constants $\{k_2, k_{-2}^0 = k_{-5}, k_5, k_{-2}^{loop}, k_p\}$ are unknown and are treated as fitting parameters in section 3.4. An unambiguous outcome of this fitting procedure is the assignment of $k_p \approx 0$, which implies $f_p \approx 0$. This outcome is anticipated by the results of section 3.1 but was not enforced during the fit procedure to the raw experimental data.

3.4. Determining the Rate Constants. The mechanism specified in eq 2 was repeatedly integrated numerically to generate predictions [U](t), [S](t), and [D](t) for the L = 716

DOI: 10.1021/acs.jpcb.7b10349
J. Phys. Chem. B 2018, 122, 1112−1120

bp, s = 482 bp DNA construct studied in Figure 2b (construct 4B-8 of ref 28). The runs were seeded with the experimental initial conditions of [U](0) = 400 nM and [E](0) = 7 nm with all other species absent at t = 0. Each integration corresponded to a different choice for the set of fit constants (k_2, $k_{-5} = k^0_{-2}$, k^{loop}_{-2}, k_5, k_p), with the remaining rate constants chosen as specified in section 3.3. To be completely clear, the integration procedure is fully general and does not enforce steady-state behavior, although the obtained results were verified to be in excellent agreement with steady-state predictions. (Deviations from steady-state behavior are, of course, observable immediately following t = 0 but extend only to times far shorter than the 5 min experimental resolution.) The fit constants were varied to identify the set that minimized the error

$$\text{Error} = \sum_{j=1}^{10} \{([S](5j\ \text{min}) - [S]_{exp}(5j\ \text{min}))^2 + ([D](5j\ \text{min}) - [D]_{exp}(5j\ \text{min}))^2\} \quad (6)$$

over all the experimental time points and both S(t) and D(t). The results of this fitting procedure are summarized in Table 1,

Table 1. Fitted Rate Constants[a]

rate constant	value
k_2	4.3×10^2 s^{-1}
k^0_{-2}, k_{-5}	1.3 s^{-1}
k_5	3.2×10^2 s^{-1}
k^{loop}_{-2}	2.1×10^7 M^{-1} s^{-1}
k_p	≈ 0 (1.7×10^{-4} s^{-1})

[a]The value of k_p is zero to within the uncertainty of the procedure but is included in parentheses just for comparison purposes. It is orders of magnitude smaller than the remaining first-order rate constants in the kinetics. If k_p = 0 is assumed and not treated as a fit constant, the remaining values of the rate constants are fit to identical values and the errors between data and best-fit predictions are negligibly changed. The data clearly describes a nonprocessive mechanism, both via comparison to the kinetic model of section 3.2 and the model-free analysis of section 3.1.

and the comparison between theoretical predictions and experimental data is found in Figure 5e. Construct 4B-8 was intentionally selected for the fitting procedure because this case was associated with high "processivity" in the original study, but the model-free analysis of section 3.1 indicates $f_p \approx 0$. Given the freedom to freely choose kinetic parameters, the system naturally evolves to a nonprocessive mechanism with k_p = 0 as a best-fit to the experimental data even in this "worst case" scenario.

The fit parameters identified in the comparison to the L = 716 bp, s = 482 bp (4B-8) DNA construct were then used without any modification to generate [U](t), [S](t), and [D](t) for the remaining "4B" constructs from ref 28 (4B-2, 4B-4, 4B-5, 4B-7, 4B-9, 4B-10; see Figure 5 for details). Note that samples 4B-1 and 4B-6 from the original study were controls, not relevant to the present work, and 4B-8 is the sample already used for the fitting procedure as described in the previous paragraph. The raw data from construct 4B-3 was misplaced and is not available for comparison, but, with that exception, the full set of data originally collected is included here and it is seen that the agreement with the proposed model is excellent. For the case of the 4B-2 construct, the new data collected in this study is shown for comparison to the simulated results (as for 4B-8). The remaining panes (b, c, d, f, and g) show data from the original study. Since this data was collected with haphazard and irreproducible time points from one repetition to the next, it was necessary to compare to single repetitions of each experiment and the loss of data quality relative to the experiments from this work is very apparent.

With the full set of rate constants in hand for each construct, eq 5 immediately predicts f_p and $(\frac{C^{S\to D}_{sp}}{C^{U\to S}_{sp}})$. Since $k_p \approx 0$, it is found that $f_p \approx 0$ for all of the constructs. The results for the specificity ratio are summarized in Table 2 along with explicit

Table 2. Inferred Values of $\frac{C^{S\to D}_{sp}}{C^{U\to S}_{sp}}$ from the Kinetic Modeling[a]

sample	L (bp)	s (bp)	$\frac{C^{S\to D}_{sp}}{C^{U\to S}_{sp}}$	$k^{loop}_{-2} \cdot J_m$ (s^{-1})	k_1 (10^7 M^{-1} s^{-1})
4B-2	368	134	0.89	1.3	3.68
4B-4	468	234	1.1	1.7	4.68
4B-5	518	284	1.3	2.1	5.18
4B-7	629	395	1.7	2.8	6.29
4B-8	716	482	1.8	2.9	7.16
4B-9	839	605	1.7	2.8	8.39
4B-10	1032	798	1.6	2.5	10.32

[a]The table also includes values of those first-order rate constants that vary from construct to construct. The remaining constants are identical over all constructs and are summarized in Table 1 and section 3.3. Note that $k_1 = k_4 = k_7$.

values for those first-order rate constants that vary from construct to construct. As expected, the looping probabilities correlate well with $(\frac{C^{S\to D}_{sp}}{C^{U\to S}_{sp}})$. Note in particular that $\frac{C^{S\to D}_{sp}}{C^{U\to S}_{sp}} = 1.8$ for the 716 bp DNA sample and $\frac{C^{S\to D}_{sp}}{C^{U\to S}_{sp}} = 0.89$ for the 368 bp DNA sample. This is in excellent agreement with the model-free analysis presented in section 3.1.

4. DISCUSSION

While the experimental data clearly indicates Dam's preference for S → D over U → S conversions, the implications of this fact are somewhat unintuitive. A distant methyl group, hundreds of bp away down the DNA chain, somehow enhances Dam's catalytic activity at the second methylation site. Although it is impossible to definitively explain the nature of this enhancement on the basis of the experiments studied here, the mechanism suggested in section 3.2 fits all of the available data very nicely. The key ingredient of this mechanism is the assumption that two competing unmethylated sites lead to some manner of interference in the turnover process, as mediated by DNA looping; this interference is not present when one of the sites has been previously methylated. For concreteness, eq 2 and Figure 4 attribute this interference to a facilitated dissociation of Dam off the target site and onto nonspecific DNA, but other schemes could presumably be written down that incorporate the looping probability between the two sites to inhibit the U → S conversion with similar results. The main qualitative points captured in the present kinetic model are (1) the nonprocessivity of the process as indicated by model-free analysis, (2) slowing of U → S conversions as s approaches the maximum in $J(s)$, and (3) little dependence of S → D velocity on s. Taken together, these three

DOI: 10.1021/acs.jpcb.7b10349
J. Phys. Chem. B 2018, 122, 1112−1120

behaviors imply a correlation between $(\frac{C_{sp}^{S\to D}}{C_{sp}^{U\to S}})$ and $J_m(s)$. While it is difficult to appreciate this correlation in the raw data (Figure 2), the effect is clearly seen when the data is plotted appropriately (Figure 3 and Table 2).

5. CONCLUSIONS

Both the model-free analysis of section 3.1 and the kinetic modeling of sections 3.2−3.4 clearly indicate nonprocessive turnover by Dam on the studied two-site DNA constructs. Our previous study[28] incorrectly attributed the observed velocity enhancement of S → D turnover relative to U → S as stemming from enzyme processivity. While the second methylation event certainly is faster than the first, the analyses carried out here (facilitated by greater precision in the new measurements) indicates the speed-up is caused by a specificity effect; Dam simply prefers S → D conversions over U → S conversions.

Beyond the specific case of Dam, this study validates the general model-free approach advocated in ref 31 and proves the practical value of such an analysis. Equation 1 and Figure 3 are clearly in excellent agreement. While an initial rates assay[10] (if possible) would presumably be able to recover the result that $f_p \approx 0$ for the studied reactions, such an analysis would completely miss the $(\frac{C_{sp}^{S\to D}}{C_{sp}^{U\to S}})$ results. At least in the case of Dam, it is the specificities and not the processivity that carry the interesting mechanistic information. It seems likely that other DNA−enzyme systems may hold similar surprises, which can be learned through the model-free analysis used here (section 3.1). If possible, kinetic studies of the modification of two-site DNAs should always be carried out to long times and sampled at regular time intervals. This allows the model-free analysis and extraction of $(\frac{C_{sp}^{S\to D}}{C_{sp}^{U\to S}})$ in addition to f_p with little additional investment beyond that required for the initial rates determination; one simply has to follow the same reaction out to longer times. Even if one only cares about f_p, fitting plots like Figure 3 to a straight line provides a statistically more reliable estimate of f_p than extracting it from a single point near $t = 0$.

A MAPPING TO A SIMPLER MODEL

The kinetic mechanism presented in section 3.2 makes a connection to familiar themes from DNA−protein interactions[9−19] involving nonspecific binding followed by translocation to the enzyme target; however, this stepwise separation is not strictly necessary from a purely kinetic viewpoint. At steady state, eq 2 approximately simplifies to the reduced effective scheme

$$\begin{array}{ccccccc} E+U & \underset{k_{-1}^{eff}(s)}{\overset{k_1^{eff}}{\rightleftharpoons}} & EU^{specific} & \xrightarrow{k_3} & E+S & & \\ & & \Big\downarrow{\scriptstyle k_{sp}} & & & & \\ E+S & \underset{k_{-4}^{eff}}{\overset{k_4^{eff}}{\rightleftharpoons}} & ES^{specific} & \xrightarrow{k_6} & E+D & \underset{k_{-7}}{\overset{k_7}{\rightleftharpoons}} & ED \end{array} \qquad (7)$$

with

$$k_1^{eff} = \frac{k_1 k_2}{k_{-1} + k_2}$$

$$k_{-1}^{eff}(s) = \frac{k_{-2}(s) k_{-1}}{k_{-1} + k_2}$$

$$k_4^{eff} = \frac{k_4 k_5}{k_{-4} + k_5}$$

$$k_{-4}^{eff} = \frac{k_{-5} k_{-4}}{k_{-4} + k_5} \qquad (8)$$

One way to derive this result has been discussed by Berg et al.[19] k_1^{eff} is calculated as the rate of formation of $EU^{specific}$ from the initial steps of the scheme appearing in eq 2:

$$E + U \underset{k_{-1}}{\overset{k_1}{\rightleftharpoons}} EU \xrightarrow{k_2} EU^{specific} \qquad (9)$$

Applying the usual steady-state arguments to eq 9, one arrives at the quoted expression for k_1^{eff}. Similarly, k_{-1}^{eff} follows from the steady-state dissociation rate predicted by the reversed reaction

$$EU^{specific} \underset{k_2}{\overset{k_{-2}}{\rightleftharpoons}} EU \xrightarrow{k_{-1}} E + U \qquad (10)$$

k_4^{eff} and k_{-4}^{eff} are calculated in an analogous fashion.

Although the effective rate constants in eq 8 are not rigorously correct for all possible values of the original rate constants, it has been verified that these results (with eq 7) are in excellent agreement with the full scheme (in eq 2) for the rate constants studied in this work. A significant advantage of the abbreviated scheme is that the kinetics follows two traditional simple Michaelis−Menten turnovers and all of the relevant constants can be inferred by simple inspection. (Detailed analysis following the methods of ref 31 leads to the same conclusions.)

$$k_{cat}^{U\to S} = k_3 + k_p$$

$$K_M^{U\to S} = (k_3 + k_p + k_{-1}^{eff}(s))/k_1^{eff}$$

$$C_{sp}^{U\to S} = k_{cat}^{U\to S}/K_M^{U\to S}$$

$$k_{cat}^{S\to D} = k_6$$

$$K_M^{S\to D} = (k_6 + k_{-4}^{eff})/k_4^{eff}$$

$$C_{sp}^{S\to D} = k_{cat}^{S\to D}/K_M^{S\to D}$$

$$f_p = \frac{k_p k_6}{(k_3 + k_p)(k_6 + k_{-4}^{eff})} \qquad (11)$$

AUTHOR INFORMATION

Corresponding Author

*E-mail: flbrown@chem.ucsb.edu. Phone: +1 (805)893-5494.

ORCID

Itay Barel: 0000-0003-2623-5900

Brigitte Naughton: 0000-0001-6233-3319

Norbert O. Reich: 0000-0001-6032-2704

Notes

The authors declare no competing financial interest.

DOI: 10.1021/acs.jpcb.7b10349
J. Phys. Chem. B 2018, 122, 1112−1120

■ ACKNOWLEDGMENTS

This work was supported in part by the National Science Foundation (CHE-1413722 and CHE-1465162).

■ REFERENCES

(1) Christmann, M.; Kaina, B. Transcriptional regulation of human DNA repair genes following genotoxic stress: trigger mechanisms, inducible responses and genotoxic adaptation. *Nucleic Acids Res.* **2013**, *41*, 8403−8420.
(2) Dominguez-Sola, D.; Ying, C. Y.; Grandori, C.; Ruggiero, L.; Chen, B.; Li, M.; Galloway, D. A.; Gu, W.; Gautier, J.; Dalla-Favera, R. Non-transcriptional control of DNA replication by c-Myc. *Nature* **2007**, *448*, 445−451.
(3) Guerra, R. F.; Imperadori, L.; Mantovani, R.; Dunlap, D. D.; Finzi, L. DNA compaction by the nuclear factor-Y. *Biophys. J.* **2007**, *93*, 176−182.
(4) Ong, C.-T.; Corces, V. G. CTCF: an architectural protein bridging genome topology and function. *Nat. Rev. Genet.* **2014**, *15*, 234−246.
(5) Ramachandran, S.; Henikoff, S. Transcriptional regulators compete with nucleosomes post-replication. *Cell* **2016**, *165*, 580−592.
(6) Sanyal, A.; Lajoie, B. R.; Jain, G.; Dekker, J. The long-range interaction landscape of gene promoters. *Nature* **2012**, *489*, 109−113.
(7) Voss, T. C.; Hager, G. L. Dynamic regulation of transcriptional states by chromatin and transcription factors. *Nat. Rev. Genet.* **2013**, *15*, 69−81.
(8) Masse, J. E.; Wong, B.; Yen, Y.-M.; Allain, F. H.-T.; Johnson, R. C.; Feigon, J. The S.cerevisiae architectural HMGB protein NHP6A complexed with DNA: DNA and protein conformational changes upon binding. *J. Mol. Biol.* **2002**, *323*, 263−284.
(9) Esadze, A.; Iwahara, J. Stopped-flow fluorescence kinetic study of protein sliding and intersegment transfer in the target DNA search process. *J. Mol. Biol.* **2014**, *426*, 230−244.
(10) Stanford, N. P.; Szczelkun, M. D.; Marko, J. F.; Halford, S. E. One- and three-dimensional pathways for proteins to reach specific DNA sites. *EMBO J.* **2000**, *19*, 6546−6557.
(11) Riggs, A. D.; Bourgeoi, S.; Cohn, M. LAC repressor-operator interaction 0.3. Kinetic studies. *J. Mol. Biol.* **1970**, *53*, 401−417.
(12) von Hippel, P. H.; Berg, O. G. Facilitated target location in biological systems. *J. Biol. Chem.* **1989**, *264*, 675−678.
(13) Lomholt, M. A.; van den Broek, B.; Kalisch, S.-M. J.; Wuite, G. J. L.; Metzler, R. Facilitated diffusion with DNA coiling. *Proc. Natl. Acad. Sci. U. S. A.* **2009**, *106*, 8204−8208.
(14) Slutsky, M.; Kardar, M.; Mirny, L. A. Diffusion in correlated random potentials, with applications to {DNA}. *Phys. Rev. E* **2004**, *69*, 61903.
(15) Shimamoto, N. One-dimensional diffusion of proteins along DNA - Its biological and chemical significance revealed by single-molecue measurements. *J. Biol. Chem.* **1999**, *274*, 15293−15296.
(16) Terry, B. J.; Jack, W. E.; Modrich, P. Facilitated diffusion during catalysis by EcoRI endonucleases. Non-specific interactions in EcoRI catalysis. *J. Biol. Chem.* **1985**, *260*, 13130−13137.
(17) Hu, T.; Grosberg, A. Y.; Shklovskii, B. I. How proteins search for their specific sites on DNA: The role of DNA conformation. *Biophys. J.* **2006**, *90*, 2731−2744.
(18) Veksler, A.; Kolomeisky, A. B. Speed-selectivity paradox in the protein search for targets on DNA: Is it real or not? *J. Phys. Chem. B* **2013**, *117*, 12695−12701.
(19) Berg, O. G.; Winter, R. B.; von Hippel, P. H. Diffusion-driven mechanisms of protein translocation on nucleic acids. 1. Models and theory. *Biochemistry* **1981**, *20*, 6929−6948.
(20) Halford, S. E. An end to 40 years of mistakes in DNA-protein association kinetics? *Biochem. Soc. Trans.* **2009**, *37*, 343−348.
(21) Sheinman, M.; Benichou, O.; Kafri, Y.; Voituriez, R. Classes of fast and specific search mechanisms for proteins on DNA. *Rep. Prog. Phys.* **2012**, *75*, 026601.
(22) Mirny, L.; Slutsky, M.; Wunderlich, Z.; Tafvizi, A.; Leith, J. S.; Kosmrlj, A. How a protein seraches for its site on DNA: the mechanism of facilitated diffusion. *J. Phys. A: Math. Theor.* **2009**, *42*, 434013.
(23) Bauer, M.; Metzler, R. Generalized facilitated diffusion model for DNA-binding proteins with search and recognition states. *Biophys. J.* **2012**, *102*, 2321−2330.
(24) Kolomeisky, A. B. Physics of protein-DNA interactions: mechanisms of facilitated target search. *Phys. Chem. Chem. Phys.* **2011**, *13*, 2088−2095.
(25) Langowaski, J.; Alves, J.; Pingoud, A.; Maass, G. Does the specific recognition of DNA by the restriction endonuclease EcoRI involve a linear diffusion step? Investigation of the processivity of the EcoRI endonuclease. *Nucleic Acids Res.* **1983**, *11*, 501−513.
(26) Porecha, R. H.; Stivers, J. T. Uracil DNA glycosylase uses DNA hopping and short-range sliding to trap extrahelical uracils. *Proc. Natl. Acad. Sci. U. S. A.* **2008**, *105*, 10791−10796.
(27) Lange, M.; Kochugaeva, M.; Kolomeisky, A. B. Protein search for multiple targets on DNA. *J. Chem. Phys.* **2015**, *143*, 105102.
(28) Pollak, A. J.; Chin, A. T.; Brown, F. L. H.; Reich, N. O. DNA looping provides for "intersegmental hopping" by proteins: A mechanism for long-range site localization. *J. Mol. Biol.* **2014**, *426*, 3539−3552.
(29) Shore, D.; Langowski, J.; Baldwin, R. L. DNA flexibility studied by covalent closure of short fragments into circles. *Proc. Natl. Acad. Sci. U. S. A.* **1981**, *78*, 4833−4837.
(30) Ringrose, L.; Chabanis, S.; Angrand, P.-O.; Woodroofe, C.; Stewart, A. F. Quantitative comparison of DNA looping in vitro and in vivo: Chromatin increases effective DNA flexibility at short distances. *EMBO J.* **1999**, *18*, 6630−6641.
(31) Barel, I.; Reich, N. O.; Brown, F. L. H. Extracting enzyme processivity from kinetic assays. *J. Chem. Phys.* **2015**, *143*, 224115.
(32) Fersht, A. *Structure and mechanism in protein science*; W. H. Freeman and Co.: New York, 1998.
(33) Cleland, W. W. Enzyme kinetics. *Annu. Rev. Biochem.* **1967**, *36*, 77−112.
(34) Cornish-Bowden, A. *Fundamentals of enzyme kinetics*, 4th ed.; Wiley-Blackwell: Weinheim, Germany, 2012.
(35) Iwahara, J.; Clore, G. M. Detecting transient intermediates in macromolecular binding by paramagnetic NMR. *Nature* **2006**, *440*, 1227−1230.
(36) Hedglin, M.; O'Brien, P. J. Hopping enables a DNA repair glycosylase to search both strands and bypass a bound protein. *ACS Chem. Biol.* **2010**, *5*, 427−436.
(37) Schonhoft, J. D.; Stivers, J. T. Timing facilitated site transfer of an enzyme on DNA. *Nat. Chem. Biol.* **2012**, *8*, 205−210.
(38) Zhou, H.-X. Rapid search for specific sites on DNA through conformational switch of nonspecifically bound proteins. *Proc. Natl. Acad. Sci. U. S. A.* **2011**, *108*, 8651−8656.
(39) Sidorova, N. Y.; T, S.; C, R. D. DNA concentration dependent dissociation of EcoRI: direct transfer or reaction during hopping. *Biophys. J.* **2013**, *104*, 1296−1303.
(40) van den Broek, B.; Lomholt, M. A.; J, K. S. M.; Metzler, R.; L, W. G. J. How DNA coiling enhances target localization bo proteins. *Proc. Natl. Acad. Sci. U. S. A.* **2008**, *105*, 15738−15742.
(41) Hedglin, M.; Zhang, Y.; O'Brien, P. J. Isolating contributions from intersegmental transfer to DNA searching by alkyladenine DNA glycosylase. *J. Biol. Chem.* **2013**, *288*, 24550−24559.
(42) Gowers, D. M.; Wilson, G. G.; Halford, S. E. Measurement of the contributions of 1D and 3D pathways to the translocation of a protein along DNA. *Proc. Natl. Acad. Sci. U. S. A.* **2005**, *102*, 15883−15888.
(43) Shimada, J.; Yamakawa, H. Ring closure probabilities for twisted wormlike chains. Application to DNA. *Macromolecules* **1984**, *17*, 689−698.
(44) Baumann, C. G.; Smith, S. B.; Bloomfield, V. A.; Bustamante, C. Ionic effects on the elasticity of single DNA molecules. *Proc. Natl. Acad. Sci. U. S. A.* **1997**, *94*, 6185−6190.
(45) Brunet, A.; Tardin, C.; Salomé, L.; Rousseau, P.; Destainville, N.; Manghi, M. Dependence of DNA persistence length on ionic

DOI: 10.1021/acs.jpcb.7b10349
J. Phys. Chem. B 2018, 122, 1112−1120

strength of solutions with monovalent and divalent salts: A joint theory-experiment study. *Macromolecules* **2015**, *48*, 3641−3652.
(46) Baumann, C. G.; Smith, S. B.; Bloomfield, V. A.; Bustamante, C. Ionic effects on the elasticity of single DNA molecules. *Proc. Natl. Acad. Sci. U. S. A.* **1997**, *94*, 6185−6190.
(47) Borochov, N.; Eisenberg, H.; Kam, Z. Dependence of DNA conformation on the concentration of salt. *Biopolymers* **1981**, *20*, 231−235.
(48) Rizzo, V.; Schellman, J. Flow dichroism of T7 DNA as a function of salt concentration. *Biopolymers* **1981**, *20*, 2143−2163.
(49) Maret, G.; Weill, G. Magnetic birefringence study of the electrostatic and intrinsic persistence length of DNA. *Biopolymers* **1983**, *22*, 2727−2744.
(50) Hagerman, P. J. Investigation of the flexibility of DNA using transient electric birefringence. *Biopolymers* **1981**, *20*, 1503−1535.
(51) Graham, J. S.; Johnson, R. C.; Marko, J. F. Concentration-dependent exchange accelerates turnover of proteins bound to double-stranded DNA. *Nucleic Acids Res.* **2011**, *39*, 2249−2259.
(52) Joshi, C. P.; Panda, D.; Martell, D. J.; Andoy, N. M.; Chen, T.-Y.; Gaballa, A.; Helmann, J. D.; Chen, P. Direct substitution and assisted dissociation pathways for turning off transcription by a MerR-family metalloregulator. *Proc. Natl. Acad. Sci. U. S. A.* **2012**, *109*, 15121−15126.
(53) Loparo, J. J.; Kulczyk, A. W.; Richardson, C. C.; van Oijen, A. M. Simultaneous single-molecule measurements of phage T7 replisome composition and function reveal the mechanism of polymerase exchange. *Proc. Natl. Acad. Sci. U. S. A.* **2011**, *108*, 3584−3589.
(54) Kunzelmann, S.; Morris, C.; Chavda, A. P.; Eccleston, J. F.; Webb, M. R. Mechanism of Interaction between Single-Stranded DNA Binding Protein and DNA. *Biochemistry* **2010**, *49*, 843−852.
(55) Luo, Y.; North, J. A.; Rose, S. D.; Poirier, M. G. Nucleosomes accelerate transcription factor dissociation. *Nucleic Acids Res.* **2014**, *42*, 3017−3027.
(56) Gibb, B.; Ye, L. F.; Gergoudis, S. C.; Kwon, Y.; Niu, H.; Sung, P.; Greene, E. C. Concentration-dependent exchange of replication protein A on single-stranded DNA revealed by single-molecule imaging. *PLoS One* **2014**, *9*, e87922.
(57) Paramanathan, T.; Reeves, D.; Friedman, L. J.; Kondev, J.; Gelles, J. A general mechanism for competitor-induced dissociation of molecular complexes. *Nat. Commun.* **2014**, *5*, 5207.
(58) Giuntoli, R. D.; Linzer, N. B.; Banigan, E. J.; Sing, C. E.; De la Cruz, M. O.; Graham, J. S.; Johnson, R. C.; Marko, J. F. DNA-segment-facilitated dissociation of Fis and NHP6A from DNA detected via single-molecule mechanical response. *J. Mol. Biol.* **2015**, *427*, 3123−3136.
(59) Tjong, H.; Zhou, H. X. DISPLAR: an accurate method for predicting DNA-binding sites on protein surface. *Nucleic Acids Res.* **2007**, *35*, 1465−1477.
(60) Wang, Y. M.; Austin, R. H.; Cox, E. C. Single molecule measurements of repressor protein 1D diffusion on DNA. *Phys. Rev. Lett.* **2006**, *97*, 048302.
(61) Elf, J.; Li, G.-W.; Xie, X. S. Probing transcription factor dynamics at the single-molecule level in a living cell. *Science* **2007**, *316*, 1191−4.
(62) Peterson, S. N.; Reich, N. O. GATC flanking sequences regulate Dam activity: evidence for how Dam specificity may influence pap expression. *J. Mol. Biol.* **2006**, *355*, 459−72.

DOI: 10.1021/acs.jpcb.7b10349
J. Phys. Chem. B 2018, 122, 1112−1120